Sensors & Actuators: B. Chemical 374 (2023) 132761

Contents lists available at ScienceDirect

Sensors and Actuators: B. Chemical

journal homepage: www.elsevier.com/locate/snb

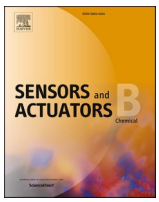

Azure A embedded in carbon dots as NADH electrocatalyst: Development of a glutamate electrochemical biosensor

Emiliano Martínez-Periñán [a,b], Aitor Domínguez-Saldaña [a], Ana M. Villa-Manso [a], Cristina Gutiérrez-Sánchez [a,b], Mónica Revenga-Parra [a,b], Eva Mateo-Martí [d], Félix Pariente [a,b], Encarnación Lorenzo [a,b,c,*]

[a] Departamento de Química Analítica y Análisis Instrumental, Universidad Autónoma de Madrid, Madrid 28049, Spain
[b] Institute for Advanced Research in Chemical Sciences (IAdChem), Universidad Autónoma de Madrid, Madrid 28049, Spain
[c] IMDEA-Nanociencia, Ciudad Universitaria de Cantoblanco, Madrid 28049, Spain
[d] Centro de Astrobiología (CSIC-INTA), Ctra. Ajalvir, Km. 4, Torrejón de Ardoz, Madrid 28850, Spain

ARTICLE INFO

Keywords:
Glutamate Biosensor
Carbon nanodot
Azure A
Glutamate dehydrogenase
NADH

ABSTRACT

Carbon nanodots modified with azure A (AA-CDs) have been synthesized and applied as redox mediator of bioelectrocatalytic reactions. A deep characterization of AA-CDs nanomaterial has been carried out, proving the covalent attachment of azure A molecules into the carbon dots nanostructure. Disposable screen-printed carbon electrodes (SPCE) have been modified with AA-CDs, through the action of chitosan polymer (Chit-AA-CDs/SPCE). The Chit-AA-CDs/SPCE electrocatalytic activity towards the oxidation of NADH has been proved, obtaining excellent results regarding the low oxidation potential achieved (−0.15 V *vs.* Ag) and low detection and quantification limits (LOD and LOQ) for NADH, 16 and 53 μM, respectively. The developed electrochemical platform has been applied for the construction of a glutamate biosensor by immobilizing L-glutamic dehydrogenase (GLDH/Chit-AA-CDs/SPCE). The morphology of GLDH/Chit-AA-CDs/SPCE platform was analysed by AFM at each different step of the electrode modification process. The resulting biosensing platform is capable of detect NADH enzymatically generated by GLDH in the presence of glutamate and NAD^+. Good analytical parameters were obtained for glutamate analysis using GLDH/Chit-AA-CDs/SPCE, as LOD and LOQ of 3.3 and 11 μM, respectively. The biosensor has been successfully applied to the analysis of food and biological samples.

1. Introduction

Glutamate is the main excitatory neurotransmitter involved in brain functions such as cognition, memory and learning. Blood glutamate levels remain in a steady state under normal conditions and a healthy diet prevents significant fluctuations, but in a variety of brain diseases, glutamate levels in either blood, cerebrospinal fluid, or both, can rise significantly, causing a serious consequence for the brain [1] and peripheral tissues [2]. Therefore, it is important to control glutamate blood level during the diagnosis of some diseases and monitoring of treatments.

Glutamate control is also important in the food industry. The ingestion of high concentrations of L-glutamate from food can induce the appearance of neurological manifestations such as Parkinson's and Alzheimer's disease [3]. Despite of these harmful effects, monosodium glutamate is one of the most widely used food-additives in commercial foods. Indeed, its use has increased over time, and it is present in many ingredients and processed foods [4]. European Food Safety Authority limits the use of glutamate as additive as a maximum permitted level of 10 g/Kg [5], which makes necessary to quantify glutamate levels in food.

The need of glutamate determination in a rapid and easy way has led to the development of alternatives to the EU official methodologies mainly based on ion exchange chromatography coupled to photometric detection (IEC-VIS). This method requires a hard sample treatment and consumes high analysis times, together with expensive instrumentation. All these reasons are leading the scientific communities to develop new analysis methods. Among them, electrochemical biosensors are capable of providing a fast response, with enough sensitivity and selectivity, and furthermore with a minimum sample treatment even in the case of

* Corresponding author at: Departamento de Química Analítica y Análisis Instrumental, Universidad Autónoma de Madrid, Madrid 28049, Spain.
E-mail address: encarnacion.lorenzo@uam.es (E. Lorenzo).

https://doi.org/10.1016/j.snb.2022.132761
Received 27 July 2022; Received in revised form 14 September 2022; Accepted 27 September 2022
Available online 30 September 2022

complex matrix, such as blood serum or food [6].

Two different enzymes have been traditionally used for glutamate biosensor development: Glutamate oxidase (GLOx) and glutamate dehydrogenase (GLDH). The fact that GLDH is usually more affordable than GLOx is the main reason why it is the favourite [6]. Furthermore, GLDH presents the advantage of a reaction mechanism independent of oxygen concentration. As GLDH is a nicotinamide adenine dinucleotide (NAD^+) cofactor dependent, the mechanism described for GLDH enzymatic reaction (1) in this kind of biosensors requires the use of a redox mediator (2), essential to carried out the electrochemical detection over the working electrode at low potentials (3):

$$L-Glutamate+NAD^{+}\xrightarrow{GLDH} \quad NADH+ \quad \alpha-ketoglutarate \tag{1}$$

$$NADH+Mediator_{ox}\rightarrow NAD^{+}+Mediator_{red} \tag{2}$$

$$Mediator_{red}\rightarrow ne^{-}+mH^{+}+Mediator_{ox} \tag{3}$$

Therefore, the development of electrochemical GLDH biosensor requires the use of redox mediator capable to electrocatalyze the oxidation of NADH. Among them, phenothiazines stand out [7,8] for the really good results obtained, in terms of the low potential required, in particular in the case of azure A (AA) [9,10].

In the way of enhancing electrochemical sensor sensitivity, nanomaterials have been widely employed with the aim of increasing the electroactive area of the working electrode, improving the signal/noise ratio [11]. In this sense, carbon nanomaterials as carbon nanotubes [12], graphene flakes [13], nanodiamonds [14] and carbon nanodots (CDs) [15–17] have been employed during the last years.

The fast and easy synthetic procedures of chemically modified CDs to endow them with specific functionalities open new possibilities of synthesizing *à la carte* nanomaterials. Bottom-up strategies allow choosing specific organic moieties that will be present in the final CDs nanostructure with the aim of providing some specific properties. This is the case of using some quinones to customize the electrochemical behaviour of CDs [18], and porphyrin-containing carbon dots, used to generate cytotoxic singlet oxygen upon irradiation, and to induce cell apoptosis [19]. Recently, our group has developed a new synthetic procedure to incorporate thionine to the CDs nanostructure, granting to CDs with electroactivity at potentials close to those described for thionine [20]. Considering the great success of AA as NADH electrocatalyst [9,10], we think that a similar approach can be carried out in order to obtain CDs with AA molecules inserted in their nanostructure, generating a material that combines the advantages of CDs and the electrocatalytic activity of AA towards NADH oxidation, with the idea of developing improved biosensors based on NADH dependent enzymes for application of different interesting analytes.

2. Materials and methods

2.1. Chemicals

Sodium chloride, dibasic and monobasic sodium phosphate, L-arginine, 3,3′-diamino-N-methyldipropylamine, azure A chloride (AA), 35% hydrochloric acid, glacial acetic acid, Chitosan, β-Nicotinamide adenine dinucleotide reduced disodium salt hydrate (NADH), β- Nicotinamide adenine dinucleotide sodium salt (oxidized form, NAD^+), L-glutamic acid monosodium salt monohydrate, bovine serum albumin (BSA), human serum and all other chemicals used in this work were purchased from Merck. L-glutamic dehydrogenase (GLDH; EC 1.4.1.3 ≥35 U/mg protein; from bovine liver) were obtained from Merck. The enzymatic assay kit for glutamate quantification (K-GLUT 04/18) was purchased from Megazyme. 0.1 M phosphate buffer (PB), pH 7.4 was prepared using 4.66 g of NaH_2PO_4 and 8.66 g Na_2HPO_4 and 1 L of Milli-Q water. Enzyme stock solution (40 U/mL) was prepared in 0.1% (w/v) BSA in 0.1 M PB, pH 7.4 and was stored at − 20 °C. All solutions were prepared using water purified with a Millipore Milli-Q-System (18.2 MΩ cm). Dialysis membrane tubing cutoff in the range of 0.1–0.5 kDa was provided by Spectrum Laboratories.

2.2. Apparatus

A CEM Discover microwave system (Matthews (NC), USA) was used for AA-CDs synthesis.

A Cary Eclipse Varian spectrofluorometer were used for fluorescence measurements. UV-Vis spectra were recorded using a UV-1900 from SHIMADZU spectrophotometer using a quartz cell.

Fourier transform infrared (FTIR) spectra were recorded from KBr pressed pellets of the solid material and precursors in the wavelength range 5000–500 cm^{-1} using a Brucker IFS60v spectrometer.

For transmission electron microscopy (TEM), Lacey carbon support film copper grids (400 mesh, Electron Microscopy Sciences) were used. Images were obtained with a JEOL JEM 2100 electron microscope.

X-ray Photoelectron Spectroscopy (XPS) analysis of the samples was carried out with a Phoibos 150 MCD spectrometer equipped with hemispherical electron analyzer, and using an Al Ka X-ray source (1486.7 eV) with an aperture of 7 mm × 20 mm. The base pressure in the ultra-high vacuum chamber was 2×10^{-9} mbar, and the experiments were carried out at room temperature. A 30 eV pass energy was applied for taking the overview sample, whereas 20 eV pass energy was applied for the analysis of the following core level spectra: O (1 s), C (1 s), and N (1 s). XPS spectra regions were fitted and deconvoluted using the fitt-xps software, calibration was done against the Au (4 $f_{7/2}$) peak set to 84.0 eV for the gold surface sample. For XPS gold AFM plates (12 mm × 12 mm, Arrandee TM Supplies, Germany) were modified.

The atomic force microscope (AFM) images were performed with an Olympus cantilever (RC800PSA, 200_20 mm) in an Agilent 5500 microscope. AFM experiments were carried out using a highly ordered pyrolytic carbon surface (HOPG).

Electrochemical experiments were performed using an Autolab PGSTAT 30 potentiostat from Metrohm-Autolab. NOVA 2.1 software package were employed. Integrated screen-printed carbon electrodes (SPCE; 4 mm diameter) from Metrohm-DropSens including a silver pseudo-reference electrode and a carbon counter electrode were used as electrochemical cells. When molecular oxygen free solutions were needed, we used a homemade single compartment cell equipped with a nitrogen purge system.

2.3. Procedures

2.3.1. Microwave assisted synthesis of Azure A carbon nanodots (AA-CDs)

AA-CDs were synthesized using 0.5 mmol of L-arginine, 0.3 mmol of AA, 0.5 mmol 3,3′-diamino-N-methyldipropylamine and 5.5 mol of Milli-Q water. The mixture was irradiated in a microwave system (CEM Discover) reaching a constant temperature of 235 °C and a maximum pressure of 20 bar during 180 s. The obtained product was dissolved in 10 mL of Milli-Q water, and the solution was filtered using 0.1 μm porous filter. Then, the obtained solution was dialyzed, using a 0.1–0.5 kDa membrane for 10 days. The resulting solution (2.25 mg/mL AA-CDs) was stored in darkness at 4 °C. Carbon nanodots without AA (CDs) were also synthesized following the same procedure (except the addition of AA) as it is reported in the literature [16].

For UV-Vis absorption and fluorescence spectroscopic characterization, equivalent concentrations of the different nanomaterials and Azure A chloride were employed. In this sense, the same amount of Azure A chloride as the used during AA-CDs synthesis (0.3 mmol) was dissolved in 150 mL of Milli-Q water. Them, before measurements, a 1/20 dilution with Milli-Q water was applied in all measured solutions. The final concentration of the three solutions under study were 0.11 mg/mL of AA-CDs, 0.11 mg/mL of CDs and 100 μM of AA in Milli-Q water.

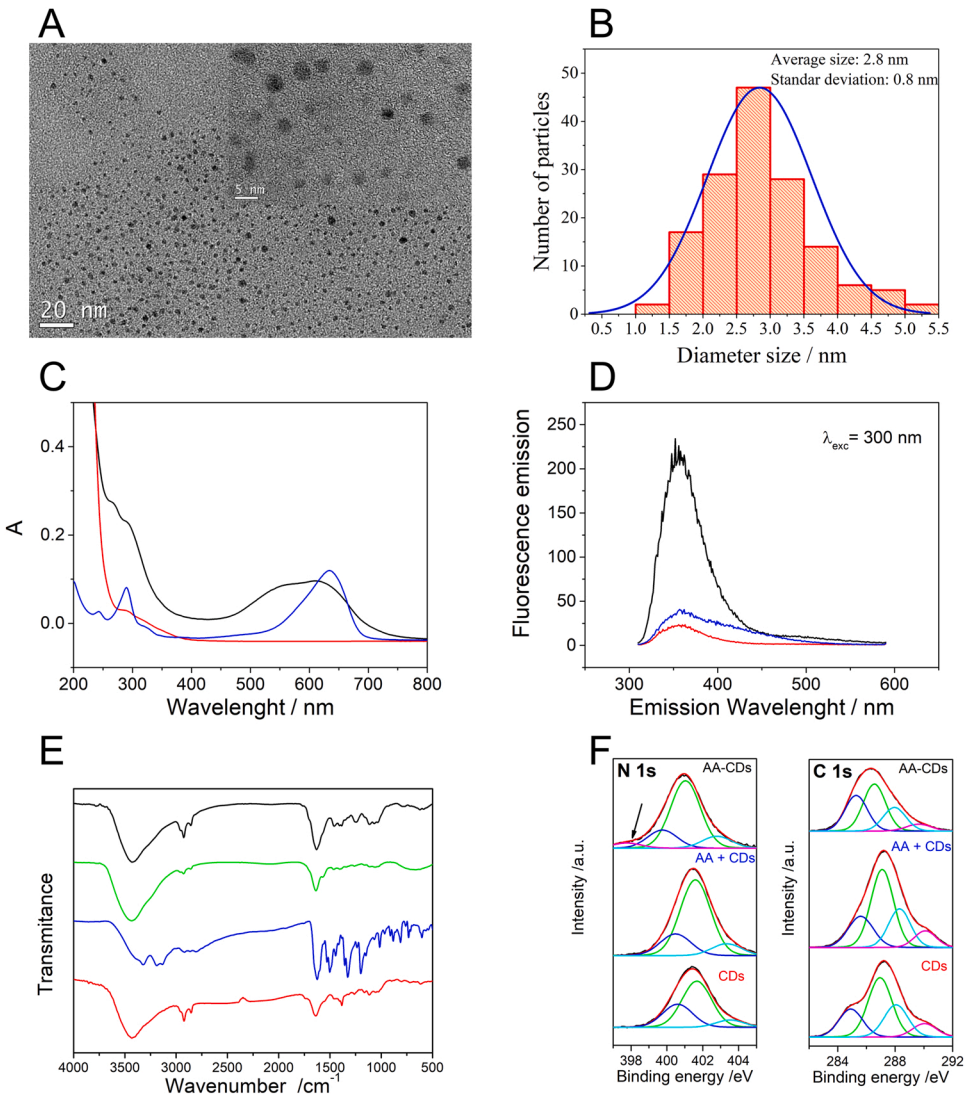

Fig. 1. (A) TEM micrograph of synthesized AA-CDs and inset with a higher magnification. (B) AA-CDs size histogram obtained from measuring 150 particles. (C) UV–Vis spectra and (D) fluorescence emission spectra (λ_{exc} = 300 nm) of 0.11 mg/mL of AA-CDs (black), 0.11 mg/mL of CDs (red) and 100 μM of AA in Milli-Q water (blue). (E) FT-IR spectra of AA-CDs (black), CDs (red), AA (blue) and a mixture of CDs and molecular AA (AA+CDs) (green). (F) XPS N 1 s and C 1 s regions of AA-CDs, CDs and AA+CDs.

2.3.2. Modification of SPCE with AA-CDs

10 μL of the AA-CDs solution (2.25 mg/mL) were drop-casted on the carbon working electrode, letting them dry at room temperature. Then, 10 μL of 1 mg/mL chitosan dissolved in 3% (v/v) glacial acetic acid were deposited in order to assure the retention of AA-CDs over the SPCE surface (Chit-AA-CDs/SPCE).

2.3.3. Glutamate biosensor preparation

10 μL of the GLDH stock solution were carefully deposited on the Chit-AA-CDs/SPCE and stored for 1 h at 4 °C to assemble the protein to the electrode surface (GLDH/Chit-AA-CDs/SPCE). Prior to use, the biosensor was rinsed with 0.1 M PB, pH 7.4 to eliminate molecules adsorbed on the electrode surface.

2.3.4. Determination of glutamate in samples

The developed amperometric biosensor was employed to determine the glutamate concentration in both blood serum and food (barbecue flavored corn snack) samples using the standard addition method. Samples of spiked human serum were used without any previous treatment other than dilution in 0.1 M PB, pH 7.4. On the other hand, 1.000 g of crushed snack was weighed, and 50 mL of water were added. To carry out the extraction of glutamate, the solution was left at 70 °C for 10 min under stirring. Then, the solution was brought to a final volume of 100.0 mL and filtered by gravity to eliminate suspended particles. Prior to chronoamperometric measurements, a 1:5 dilution in 0.1 M PB, pH 7.4 was carried out. The results obtained were validated towards a commercial spectrophotometric enzymatic assay kit used following the procedure described by the manufacturer.

3. Results and discussion

3.1. Synthesis and characterization of Azure A carbon nanodots (AA-CDs)

TEM images (Fig. 1(A)) show the quasi-circular shape of AA-CDs. The average diameter size obtained from the measurement of 150 particles was 2.8 nm with a standard deviation of 0.8 nm (Fig. 1(B)). The AA-CDs show diameter ranging from 1.0 until 5.5 nm. No aggregates were observed.

The UV-Vis spectrum (Fig. 1(C)) of AA-CDs (black line) shows an absorption peak at 285 nm related to π-π * transition of the conjugated C═C present in the CDs core. This contribution can also be observed in the CDs spectrum (red line). A band around 300 nm appears in the AA-CDs spectrum associated with the π-π * transition of the phenothiazine ring as it can be also observed in the AA spectrum (blue line). In the AA spectrum, a maximum at 635 nm associated with a vibrational band assigned to the n–π * transitions of the C═N bond of the phenothiazine ring is also observed. The peak ascribed to the AA covalently inserted in

the carbon nanodots structure (AA-CDs, black line) can be identified as a broad band with two peaks contribution at 560 and 614 nm. As can be deduced both peaks are close to the peak associated with the phenothiazine ring of AA, but they are shifted because of the generation of different covalent bonds that attach the ring into the AA-CDs nanostructure. Other experiment that points out the insertion of phenothiazine ring in the carbon nanodots structure is the fluorescence emission. As can be observed in the fluorescence spectra (Fig. 1(D)), AA-CDs (black), CDs (red) and AA (blue) solutions emit light at 360 nm when are excited with 300 nm wavelength radiation. However, the emission is quite more intense in the case of AA-CDs compared with CDs and AA (in equivalent concentration). This effect can be attributed to the presence of phenothiazine rings inserted in the carbon nanostructure.

In order to confirm the composition of the new synthesized AA-CDs, elemental analysis was carried out. Results indicate 52.58% C, 8.12% H, 20,78% N, 1.44% S and 17.08% O (calculated). The data obtained for non-modified CDs are 50.29% C, 9.04% H, 21.93% N, 0.00% S and 18.74% O (calculated). As can be expected the presence of S in the case of AA-CDs is a consequence of the insertion of the phenothiazine, since S is not found in the unmodified CDs, being this result other evidence of the presence of the AA in the AA-CDs nanostructure.

To confirm the insertion of AA molecules in the AA-CDs nanostructure, and to discard the just adsorption of phenothiazine on CDs, FT-IR spectrum of AA-CDs were analyzed and compared with the spectrum obtained for AA, unmodified CDs and a mixed of AA and unmodified CDs (AA+CDs) (Fig. 1(E)). AA spectrum (blue line) shows a band around 3324 cm^{-1} related to primary amines, bands at 2863, and 2919 cm^{-1} derived from the C-H bond stretching vibration, bands at 1654, 1500, 1326, 1203 and 604 cm^{-1} due to secondary aromatic amines and bands at 813 and 882 cm^{-1} related to the thioether of the phenothiazine ring. Unmodified CDs spectrum (red line) shows bands at 1639 and 896 cm^{-1} associated with aromatic amines and the band at 802 cm^{-1} with secondary amine, all of them due to L-Arginine precursor, in addition to bands at 3432, 1639 and 1116 cm^{-1} (primary amines) and the band at 1166 cm^{-1} (tertiary amine) coming from 3,3′-diamino-N-methyldipropylamine. The FT-IR spectrum of CDs also shows the stretching band of OH and NH_2 as a broad band centered at 3423 cm^{-1}, the bands around 2915 and 2847 cm^{-1} derived from the C-H bond stretching vibration; C═O stretching vibrations appears at 1560 cm^{-1}. At 1644 cm^{-1} appears a band ascribed to the C═N stretching, while the bands at 1457 cm^{-1} and 1384 cm^{-1} are related to C-N bonds. The 1080 cm^{-1} band correspond to the alcoxy (C-O) stretching vibrations. The AA-CDs FT-IR spectrum (black line) shows the bands of CDs besides the main bands observed for AA at 1654, 1500 and 1203 cm^{-1}, but with a higher intensity. These results and the difference with the spectrum of the mixture (AA+CDs, green line). In particular, the band around 1628 cm^{-1}, consequence of the C═N stretching, agree well with the insertion of phenothiazine rings in the AA-CDs nanostructure rather than a simple adsorption happening at AA+CDs by the generation of imide groups. At the same time the band at 2926 cm^{-1} is ascribed to N-H stretching, probably due to the generation of aldimine groups when Azure A is covalently attached into the carbon nanodots structure.

Complementary, XPS analysis of the AA-CDs, AA+CDs and CDs was performed to corroborate the successful insertion of AA in the CDs structure. Fig. 1(F) shows the N 1 s and C 1 s core level peaks of the AA-CDs (covalent linkage), AA+CDs and CDs samples. High-resolution spectrum of nitrogen shows complex features, which were carefully decomposed. A best-fit of the N 1 s core level shows three contributions at c.a. 400.5–400.0 eV, 401.1–401.66 eV and 403.0–403.5 eV, which are assigned to nitrogen in N-(C3), C═N (cycles) and N═C positive charges (quaternary) species, respectively [21]. It is remarkable that the AA-CDs compound presents an extra forth nitrogen component at 397.9 eV, which would be assigned to the pyridinic nitrogen (imine) structure [21–23], that is, to nitrogen with alone electron pair, located either at the edge of the graphitic network or next to a vacancy, and bonded to two carbon atoms. The presence of an additional component

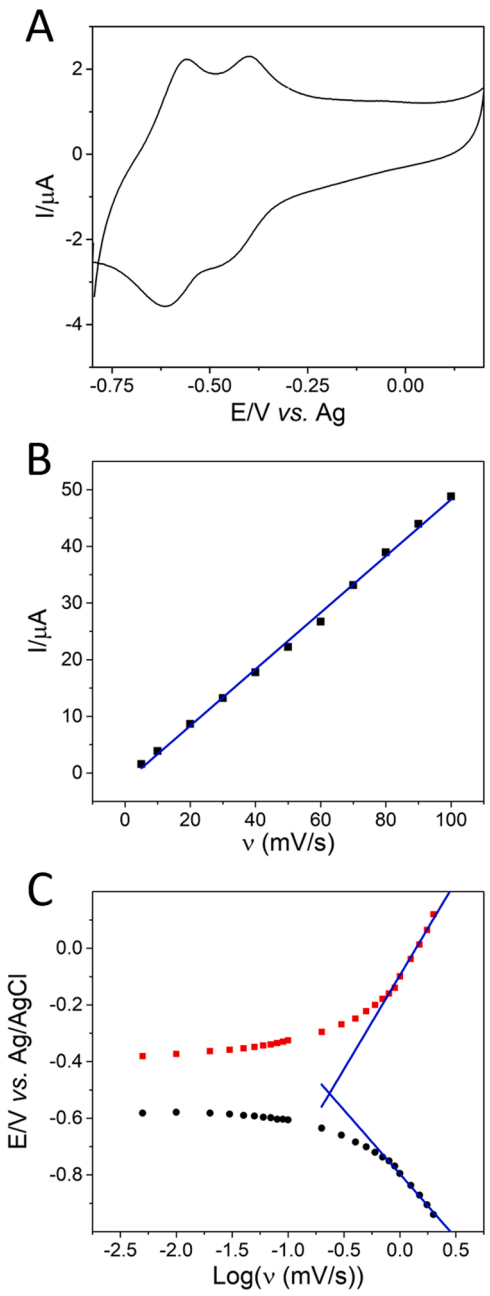

Fig. 2. (A) Cyclic voltammetric response of Chi-AA-CDs/SPCE at 10 mV/s in 0.1 M PB, pH 7.4. (B) Oxidation peak current *vs* scan rate of the process at $E^0 = -0.63$ V. (C) Laviron's plot showing the dependence of the peak potential on the logarithm of scan rate of the process at $E^0 = -0.63$ V.

only for the AA-CDs (covalent linkage sample) suggests a chemical structure modification, compatible with a covalent interaction between the dye AA and the CDs, which does not appear in the AA+CDs case. Therefore, the XPS data confirm the results described above, indicating the covalent insertion of AA on the nanodots (AA-CDs), whereas for the AA+CDs mixture does not occur. Additionally, the C 1 s peak for the AA-CDs shows noteworthy changes in its shape respect to the CDs and AA+CDs (see Fig. 1(F) C 1 s). Although the C 1 s core level peak presents four similar components at 285.2 eV, 286.8 eV, 288.2 eV and 289.9 eV for all cases, the ratio between the components is different for the AA-CDs. Whereas CDs and AA+CDs show a very similar peak profile for the carbon region, the AA-CDs shows a remarkable increase of the first carbon component. This fact is in good agreement with the chemical modification described above for the AA-CDs.

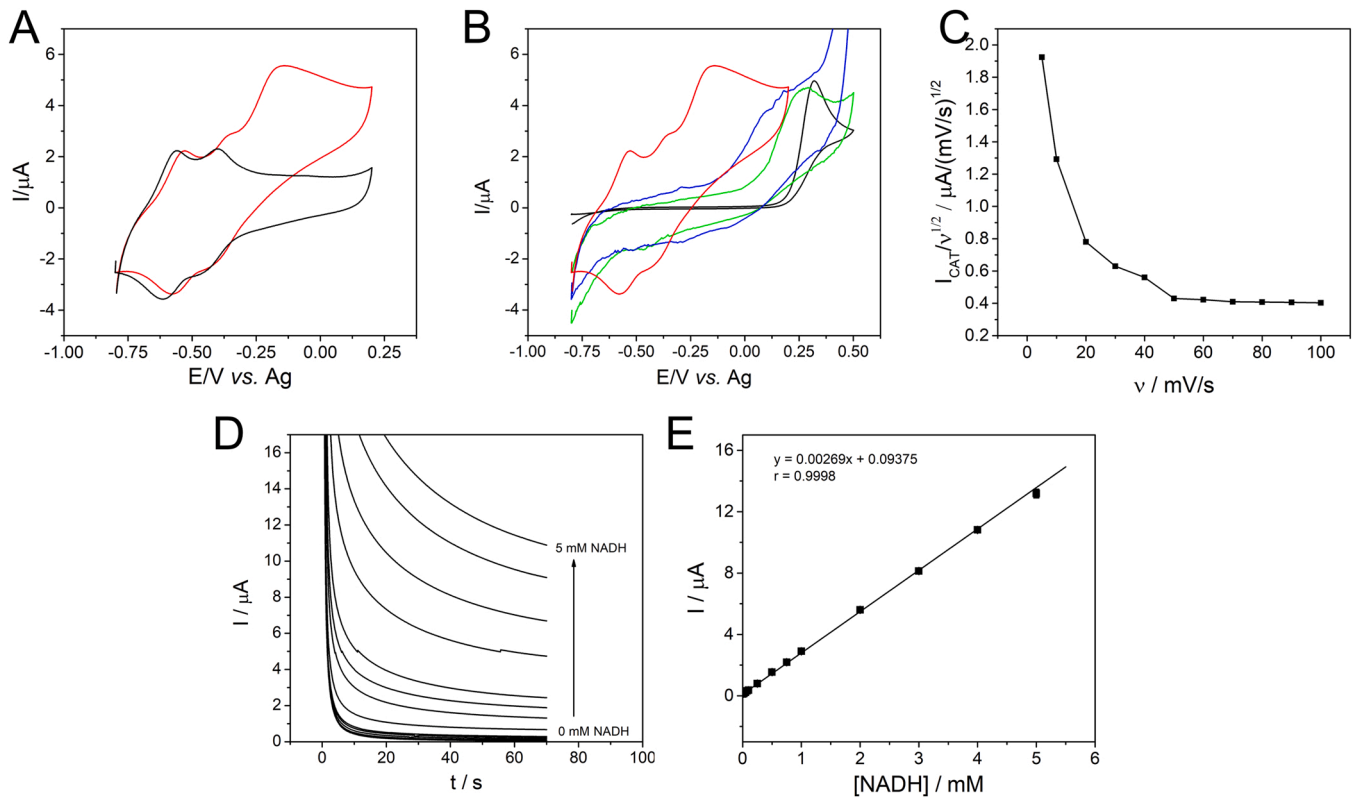

Fig. 3. (A) Cyclic voltammetric responses at Chi-AA-CDs/SPCE in the absence (black) and in the presence of 1.0 mM NADH (red) in 0.1 M PB, pH 7.4 at 10 mV/s. (B) Cyclic voltametric responses at Chi-AA-CDs/SPCE (red), Chi-CDs/ SPCE (blue), Chi/ SPCE (green) and SPCE (black) in the presence of 1.0 mM NADH in 0.1 M PB, pH 7.0 at 10 mV/s. (C) Plot of the normalized catalytic peak current ($I_{CAT}/v^{1/2}$) with the scan rate in the presence of 1.0 mM NADH using Chi-AA-CDs/SPCE. (D) Chronoamperometric measurements using Chi-AA-CDs/SPCE at E_{ap} = 0.0 V *vs* Ag in 0.1 M PB, pH 7.0 at increasing NADH concentrations. (E) Calibration plot obtained for NADH determination with AA-CDs/SPCE using chronoamperometry and measuring the steady state current at 60 s.

In summary, FT-IR and XPS complementary techniques prove a remarkable difference between AA-CDs and AA+CDs, confirming the interaction between the due AA and the CDs in both cases (AA+CDs and AA-CDs), and the effective covalently insertion of AA in the CDs structure in the case of AA-CDs.

3.2. Electrochemical characterization of AA-CD modified electrodes

SPCEs modified with AA-CDs (Chit-AA-CDs/SPCE) as described in the experimental section were electrochemically tested in 0.1 M PB, pH 7.4. The cyclic voltammogram (CV) (Fig. 2(A)) shows two redox couples at formal potentials of −0.45 and −0.63 V *vs.* Ag. These redox couples are associated with the oxidation and subsequent reduction of AA [24]. From the Tafel slope, it can be determined that the number of electron exchange during each redox process is one. In the bibliography it is reported that AA immobilized on the electrode surface exchange two electrons in a single redox process [10,25]. The unfolding of this process in two redox process of a single electron each is probably due to the modification of AA phenothiazine ring covalently inserted in the AA-CDs nanostructure, being considered another evidence of the CDs modification. The surface coverage (Γ) of Chit-AA-CDs/SPCE can be evaluated from the CV using the equation $\Gamma = Q_{Ox}/nFA$, where Q_{Ox} is the charge obtained after integration of the oxidation peak ($E^0 = -0.63$ V), F is the Faraday constant (96,485 C/mol), n is the number of electrons transferred in the redox process (n = 1) and A is the area of the electrode (0.13 cm^2). The Γ value was calculated to be (23.9 ± 0.2) pmol/cm^2.

In order to characterize the electrochemical process, the oxidation peak current intensity of the redox couple at $E^0 = -0.63$ V were analyzed *vs.* the scan rate (*ν*) (Fig. 2(B)). As can be observed, the correlation between both parameters is lineal, which implies that it is a surface confined electron transfer process. This was an expected result as AA-CDs are immobilized on the SPCE working electrode surface through the chitosan polymer avoiding the loss of nanomaterial.

Once it has been proved that the redox process is non-diffusional, the apparent electron-transfer rate constant (k_s), as well as the electron-transfer coefficient (α) have been determined through the Laviron's equations. The anodic and cathodic peak potentials have been plotted *vs.* log (*ν*) in a typical Laviron's plot (Fig. 2(C)). From the ratio of the slopes of these straight lines, the electron-transfer coefficient (α) and the apparent electron-transfer rate constant (k_s) have been determined as 0.60 and 4.7 s^{-1}, respectively.

3.3. Electrocatalysis of NADH

The electrocatalytic activity of the Chit-AA-CDs/SPCE were tested using CV at 10 mV/s (Fig. 3(A)). As has been described previously, in the absence of NADH (black line) two redox pairs are observed (E^0 =−0.45 V and E^0 =−0.63 V *vs.* Ag). However, when 1.0 mM NADH is present in the solution, a third peak just at the end of the more positive one appears, increasing its current intensity as the NADH concentration increases. This new oxidation wave corresponds to the electrocatalytic oxidation of NADH by AA-CDs, which in this case presents a slow kinetic. Despite of the slow rate of the process, the potential at − 0.15 V *vs.* Ag is quite low to carry out the electrooxidation of NADH compared with an unmodified electrode, or an electrode modified with CDs (not containing AA molecules covalently linked to their structure) as can be observed at Fig. 3(B). The electrochemical mechanism determined using Nicholson and Shain's theory, points out an electrocatalytic ECE reaction, as it is deduced from the shape of the normalized catalytic peak current with square root of scan rate ($I_{CAT}/v^{1/2}$) *vs.* cyclic voltammetry scan rate (*ν*) plot in the presence of 1.0 mM NADH (Fig. 3(C)).

The amount of AA-CDs used to modify SPCE was optimized (Fig. S1

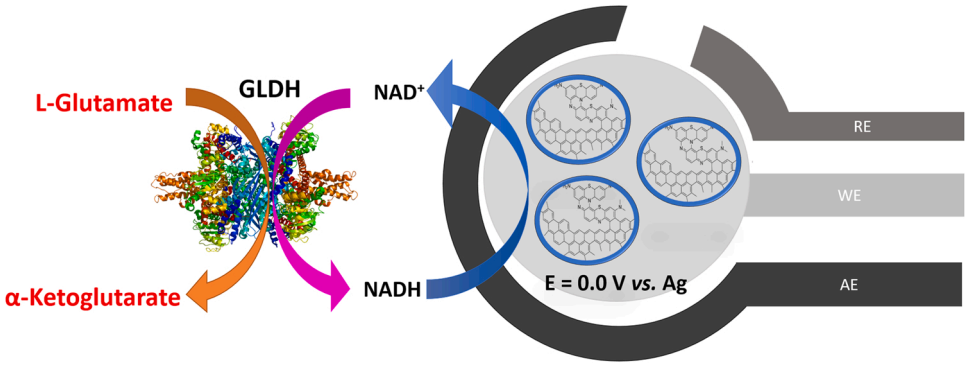

Scheme 1. L-glutamate Biosensor.

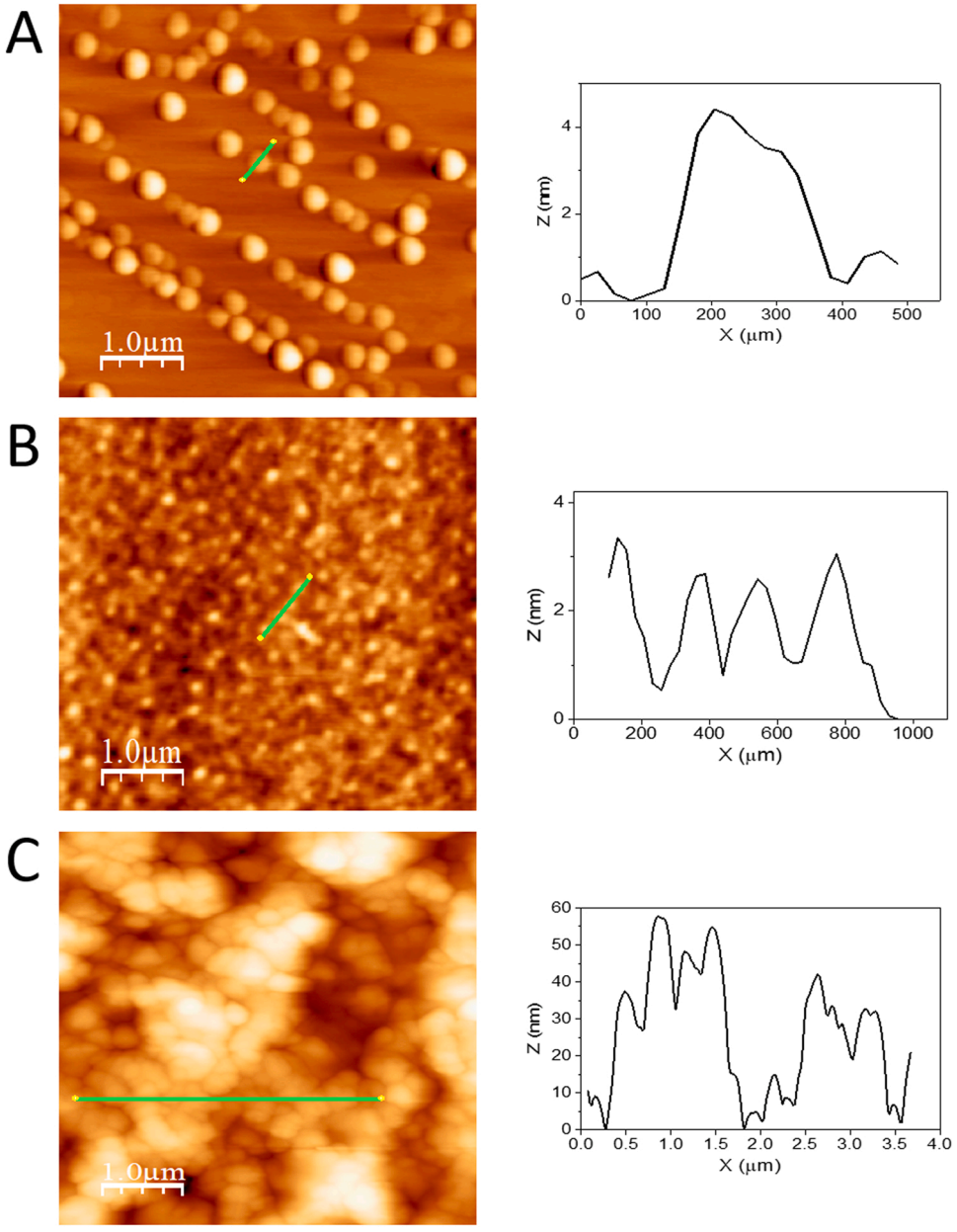

Fig. 4. AFM topographic images and the corresponding topographic profile of: (A) AA-CDs-HOPG, (B) Chit/AA-CDs-HOPG and (C) GLDH/Chit/AA-CDs-HOPG.

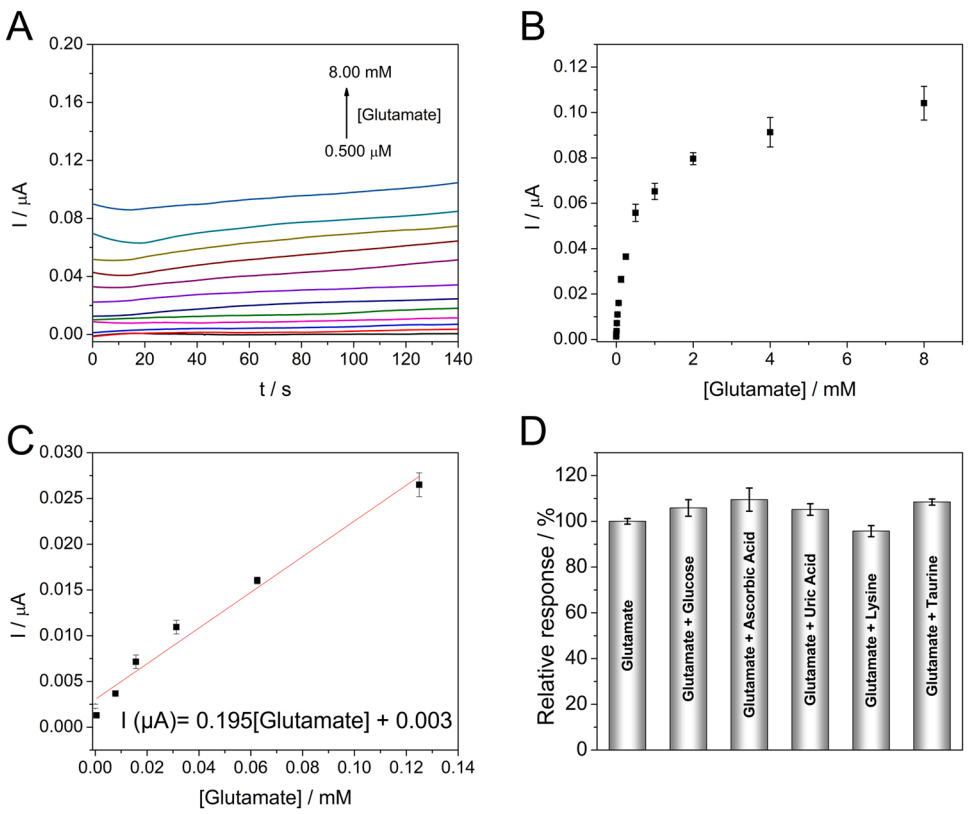

Fig. 5. (A) Chronoamperometric response (E_{ap}= 0.0 V *vs* Ag) of the biosensor (GLDH/Chit-AA-CDs/SPCE) in 0.1 M PB, pH 7.4 containing 10.0 mM NAD^+ after the addition of increasing amounts of glutamate. (B) Calibration curve obtained from (A). (C) Concentration linear range from (B). (D) Relative response of the biosensor to 0.10 mM L-glutamate measured in the presence of potentially interfering compounds at the concentration of 0.10 mM. The data presented are the average value of three determinations.

(A)) trying to obtain the highest electrocatalytic current in the CV experiment in the presence of 1.0 mM NADH in the solution. As can be observed, the chosen volume of the 2.25 mg/mL AA-CDs suspension was 10 μL as the electrocatalytic current does not increase when higher volumes of the suspension were deposited on the working electrode surface. The amount of 1.0 mg/mL chitosan solution employed to attached AA-CDs onto the working electrode surface was also optimized (Fig. S1(B)). In this case, we had to establish a compromise between the intensity of the catalytic peak and the stability of the biosensor in successive potential scans, choosing as best 10 μL of the chitosan solution.

We have used this electrocatalytic effect to develop an electrochemical sensor for NADH. Chronoamperometric curves at constant potential of 0.0 V *vs.* Ag (approx. 60 mV after the NADH electrooxidation peak process) (Fig. 3(D)) showed that the steady state current increases proportionally to the NADH concentration (Fig. 3(E)). The figures of merit of the developed sensor were a lineal range from 53 to 5000 μM and a sensitivity of 2.7 μA/mM. The LOD and LOQ were calculated as the concentration of analyte that gave a signal equal to 3 and 10 times the standard deviation of background current, respectively, obtaining values of 16 μM and 53 μM as LOD and LOQ, respectively.

The catalytic constant (k_{CAT}) for the reaction between NADH and the adsorbed AA-CDs was evaluated by chronoamperometry using the procedure described by Galus [26]. A value of 1.57×10^3 M^{-1} s^{-1} was found to be, which is higher than other previously reported by our group for nanodiamonds modified by electrografting with AA [14], and in the same order of the best NADH sensors described based on the direct electrografting of AA on SPCE [10] and on graphene oxide nanolayers [9].

3.4. L-glutamate biosensor

A step forward has been carried out based on the results above described, using the Chit-AA-CDs/SPCE platform to develop a glutamate electrochemical biosensor. The biosensor is based on the detection of the NADH generated in the enzymatic reaction by GLDH in the presence of NAD^+ at different concentrations of glutamate. In the reaction, L-glutamate is enzymatically transformed into α-ketoglutarate (see Scheme 1). The GLDH based biosensor was developed immobilizing the enzyme on the Chit-AA-CDs/SPCE as described in the experimental section.

AFM topography analysis has been employed to follow the different steps of the biosensor development. SPCE is a very rough surface. Hence, in order to get an adequate carbon planar surface suitable for AFM studies, we employed HOPG planar electrode. Fig. 4(A) shows a topographic AFM image of HOPG surface after dropping the solution containing AA-CDs. The surface is partially covered with circular structures, generating a straight-line distribution of AA-CDs. After chitosan deposition (Fig. 4(B)), the surface is completely coated with the polymer and AA-CDs can be seen through the chitosan polymer network. In this arrangement, AA-CDs are randomly distributed around the surface, not only preferably deposited over the HOPG plane edges, which is a consequence of their hydrophilic nature, what justified their random distribution around the polymer network. Finally, after GLDH immobilization on Chit/AA-CDs-HOPG (Fig. 4(C) the surface is completely covered by globular structures associated with GLDH. The height profile suggests that the enzyme is organized into multiple layers, which is an advantage when designing a biosensing platform.

Cyclic voltammetry was employed to follow the respond of the developed biosensor in the presence of glutamate. Fig. S2(A) shows the CV response of GLDH/Chit-AA-CDs/SPCE in the absence and in the presence of 1 mM glutamate in the presence of the cofactor NAD^+. As in the case of NADH sensor (Chit-AA-CDs/SPCE), the third peak ascribed to NADH electrooxidation appears, showing the proper activity of GLDH transforming L-glutamate into α-ketoglutarate and generating NADH. In order to study the effects of all biosensor components, control experiments were carried out (Fig. S2(B)). No L-glutamate detection occurs using electrodes without AA-CDs. Furthermore, the response is quite low in the absence of chitosan, which is the responsible of retaining AA-CDs

Table 1
Comparison of previously reported amperometric glutamate biosensors based on glutamate dehydrogenase and glutamate oxidase.

Electrode	Enzyme	E (V) *vs.* NHE	Linear Range (μM)	LOD (μM)	Ref.
MB-p-DAB/ SWCNTs/GCE	Glutamate dehydrogenase	0.197	0 – 100	2	[27]
MB-CHIT/GCE	Glutamate dehydrogenase	0.097	–	2	[28]
Naf/GLDH-bacteria/PEI-MWNTs/GCE	Glutamate dehydrogenase	0.761	10 – 1,000; 2,000 – 10,000	2	[29]
MWCNTs-CHIT-MB/GLDH-NAD^+-CHIT-MB/MWCNTs-CHIT-MB/MB-SPCE	Glutamate dehydrogenase	0.297	7.5 – 105	3	[30]
OA-CPE	Glutamate dehydrogenase	0.547	400 – 10,000; 10,000 – 100,000	100	[31]
CHIT-MB-/SPCE	Glutamate dehydrogenase	0.297	12.5 – 150	1.5	[32]
Th–SWNTs/GCE	Glutamate dehydrogenase	0.190	0.5 – 400	0.1	[33]
GluOx/cMWCNT/ AuNP/CHIT/ AuE	Glutamate oxidase	0.332	5–500	1.6	[34]
GluOx/Au NPs/ GO/CHIT/AuE	Glutamate oxidase	0.447	200–1,400	23	[35]
GluOx-BSA/ PPYox/ SPPtE	Glutamate oxidase	0.897	5–1,000	1.8	[36]
GluOx/CHIT/ AuNPs/PBNCs/ rGO-Pt	Glutamate oxidase	0.697	0.05–40	0.04	[37]
GluOx/ PPYox/ Pt-MWCNTs/ GC	Glutamate oxidase	0.697	10–100	0.88	[38]
GLDH/Chit-AA-CDs/SPCE	Glutamate dehydrogenase	0.197	11 – 125	3.3	This work

over the electrode surface, avoiding their migration into the bulk solution and assuring a great electrocatalytic activity and the proper L-glutamate detection.

In order to obtain the best biosensor response, the amount of enzyme used in the construction of the biosensor was optimized. In this sense, biosensors with increasing amounts of GLDH were prepared and their chronoamperometric response at 0.0 V *vs.* Ag in the absence (I_o) and in the presence of 0.5 mM glutamate and 10.0 mM NAD^+ (I_{glut}) were recorded (Fig. S3(A)). The ratio I_{glut}/I_o increases as the units of enzyme included in the biosensing layer increase up to 0.4 U (10 μL of 40 U/mL). For enzyme loadings higher than 0.4 U, a decrease in the ratio I_{glut}/I_o is observed suggesting that there is an excess of enzyme on Chit-AA-CDs/SPCE, which would cause a hindrance to charge transfer towards the electrode surface. Hence, 0.4 U were selected as the optimal amount of enzyme.

In addition, the effect of the buffer solution pH (from 6.0 to 8.0) on the biosensor response was evaluated. The ratio I_{glut}/I_o increases on increasing pH up to 7.4 and then decreases (Fig. S3(B)). Considering this result, the following electrochemical measurements were carried out using 0.1 M PB, pH 7.4.

Once the work conditions were optimized, the high electrocatalytic response mediated by AA-CDs was corroborated by recording the biosensor chronoamperometric response at 0.0 V *vs.* Ag to increasing glutamate concentrations in the presence of 10.0 mM NAD^+ (Fig. 5(A)). The biosensor (GLDH/Chit-AA-CDs/SPCE) current response increases on increasing glutamate concentration, following the typical Michaelis-Menten behavior (Fig. 5(B)), which confirms that the analytical response is controlled by the enzymatic reaction. From the linear part of the calibration plot, the figures of merit of the glutamate biosensor were obtained. It was observed that the biosensor response presents a good linearity with the glutamate concentration up to 125 μM (Fig. 5(C)), with a sensitivity (calculated from the slope of the plot) of 0.20 ± 0.02 μA/mM. Detection and quantification limits of 3.3 and 11 μM, respectively, were estimated as indicated above. These analytical parameters compare well to those obtained for other amperometric glutamate dehydrogenase and glutamate oxidase based biosensors (Table 1) with the advantage that in our work the oxidation of the glutamate takes place at lower potential. In addition, the reproducibility of the proposed biosensor was evaluated comparing the analytical signals obtained using three different devices prepared in the same manner and a value of RSD lower than 7% was obtained.

The storage stability of the biosensor stored at 4 °C was evaluated by measuring the chronoamperometric response of 0.5 mM glutamate in the presence of 10.0 mM NAD^+. The response retained more than 85% of the initial signal after 2 weeks storage as can be seen in Fig. S4. The operational stability of the biosensor was also studied. The chronoamperometric response of the biosensor was recorded for successive measures of 0.5 mM glutamate. The current values are the same for more than 30 consecutive measurements (Fig. S5 (A)). Furthermore, the biosensor response under continuous hydrodynamic conditions was evaluated by setting a constant potential of 0.0 V and monitoring the current intensity. Fig. S5 (B) clearly shows a constant current, pointing out a good operational stability of GLDH/Chit-AA-CDs/SPCE under continuous operation.

Selectivity is a key parameter in the development of enzymatic biosensors focused on the analysis of biological or food samples. For this reason, the effect of potential interfering compounds that might affect the biosensor response was investigated. Fig. 5 (D) shows the relative response as the ratio between the biosensor responses to 0.10 mM glutamate in the absence and in the presence of different potential interfering substances such as glucose, ascorbic acid, uric acid, lysine, and taurine that may be present in the samples. As can be seen, there is no significant effect in the response for all the compounds assayed at the same concentration of the analyte (0.1 mM), demonstrating that the biosensor (GLDH/Chit-AA-CDs/SPCE) can be used for the selective determination of glutamate. To assure that the biosensor respond is specific to glutamate, an interference study was also carried out in the presence of high concentration (0.5 mM) of potential interfering compounds. Results clearly showed no effects of the potential interfering compounds on the biosensor response (see Fig. S6) even at high concentrations.

MB: meldola blue, p-DAB: poly-1,2-diaminobenzene, SWCNTs: Single-walled carbon nanotubes, GCE: glassy carbon electrode, CHIT: chitosan, Naf: nafion, GLDH-bacteria: bacteria surface-displayed glutamate dehydrogenase, PEI: polyethyleneimine, MWCNTs: multiwalled carbon nanotubes, SPCE: screen-printed carbon electrode, OA: octadecylamine, CPE: carbon paste electrode, Th: thionine, GluOx: Glutamate oxidase, cMWCNT: carboxylated multi walled carbon nanotubes, AuNP: gold nanoparticles, GO: Graphene oxide, SPPtE: screen printed platinum electrodes, PPYox: overoxidized polypirrole, PBNCs: Prussian blue nanocubes, Pt-MWCNTs: multiwalled carbon nanotubes decorated with Pt nanoparticles.

3.5. *L-glutamate analysis in food and biological samples*

To demonstrate the applicability of the developed biosensor, it was applied to the glutamate determination in both food and biological samples. Specifically, it was determined the amount of glutamate present in a corn snack, and, on the other hand, the recovery obtained after adding the analyte to a commercial human serum. Prior to the determination, samples were pretreated as described in the experimental section. In both cases, the standard addition method was used in order to minimize matrix effects. Moreover, the results obtained with the enzymatic biosensor were compared with those obtained with a commercial

Table 2
Determination of glutamate in different samples with the enzymatic biosensor and with a commercial enzymatic kit.

	Enzymatic biosensor				Enzymatic biosensor		Enzymatic kit	
	Added	Found	Recovery		Found	RSD	Found	RSD
Sample	(μM)	(μM)	(%)	Sample	(μM)	(%)	(μM)	(%)
Serum (n = 3)	37.5	39 ± 3	104	Snack (n = 3)	215 ± 6	2.8	218 ± 9	4.1

enzymatic kit for the determination of glutamate to validate the proposed biosensing method.

The matrix effect on the biosensor response was evaluated by comparing calibration plots obtained in 0.1 M PB, pH 7.4 or by standard addition in spiked human serum or snack sample (Fig. S7). As one would expect according to the complexity of the matrix, barely different exist between the slopes in the case of the serum sample but the differences are significant in snack sample. Despite of that, the results summarized in Table 2 show the good recovery obtained by triplicated in the analysis of the serum spiked with a known amount of the analyte. In the case of the snack sample, the glutamate found value agrees well with that obtained with a commercial spectrophotometric enzymatic kit used as reference method. These results confirm the suitability of the proposed methodology for an adequate and accurate determination of glutamate in both biological and food samples, without the need of time-consuming pretreatment of the sample.

4. Conclusions

New AA-CDs nanomaterial has been synthesized and characterized proving the insertion of AA in the CDs nanostructure through covalent attachment. The electrocatalytic effect of AA molecules for NADH electrooxidation is inherited by the carbon nanodots, improving even the described electrooxidation potentials for AA molecules attached over electrode surfaces. This great electrocatalytic behavior has been taken in advantage to develop initially a NADH sensor platform (Chit-AA-CDs/SPCE) and in a second step a glutamate biosensor platform (GLDH/Chit-AA-CDs/SPCE) immobilizing GLDH enzyme over the modified electrode surface. Both platforms have shown great sensitivity and low LOD and LOQ for both NADH and L-glutamate determination. Finally, the developed L-glutamate biosensor has been successfully applied to analyze glutamate in food and biological samples.

Funding

This work has been supported by the Spanish Ministerio de Ciencia e Innovación (PID2020–116728RB-I00) and Comunidad Autónoma de Madrid (SI3/PJI/2021–00341, P2018/NMT-4349 TRANSNANOAVANSENS Program).

CRediT authorship contribution statement

Emiliano Martínez-Periñán design the experiments, conceptualized the synthesis of azure A carbon nanodots, characterized them and proposed their used as NADH electrocatalyst. **Aitor Domínguez-Saldaña** did the experiments to develop NADH sensor, **Ana M. Villa-Manso** did the experiment to develop glutamate biosensors, **Cristina Gutiérrez-Sánchez** did AFM experiments, evaluated the results and prepare the manuscript, **Mónica Revenga-Parra** designed the experiments and manuscript, **Eva Mateo-Martí** carried out XPS experiments and evaluated the results proposing valuable information about AA-CDs synthesis, **Félix Pariente** designed the experiments, **Encarnación Lorenzo** conceived the overall idea and concept.

Declaration of Competing Interest

The authors declare that they have no known competing financial interests or personal relationships that could have appeared to influence the work reported in this paper.

Data Availability

Data will be made available on request.

Acknowledgements

We would like to thank Santos Gálvez-Martínez for his collaboration in XPS measurements. This work has been supported by the Spanish Ministerio de Ciencia e Innovación (PID2020–116728RB-I00) and Comunidad Autónoma de Madrid (SI3/PJI/2021–00341, 2021–5A/BIO-20943 and P2018/NMT-4349 TRANSNANOAVANSENS Program).

Appendix A. Supporting information

Supplementary data associated with this article can be found in the online version at doi:10.1016/j.snb.2022.132761.

References

[1] S.-J. Yang, E.-A. Kim, M.-J. Chang, J. Kim, J.-M. Na, S.Y. Choi, S.-W. Cho, N-Adamantyl-4-Methylthiazol-2-Amine attenuates glutamate-induced oxidative stress and inflammation in the brain, Neurotox. Res. 32 (2017) 107–120, https://doi.org/10.1007/s12640-017-9717-x.
[2] Z.-H. Wen, Y.-C. Chang, Y.-H. Jean, Excitatory amino acid glutamate: role in peripheral nociceptive transduction and inflammation in experimental and clinical osteoarthritis, Osteoarthr. Cartil. 23 (2015) 2009–2016, https://doi.org/10.1016/j.joca.2015.03.017.
[3] M.I.P. Oliveira, M.C. Pimentel, M.C.M. Montenegro, A.N. Araújo, M.F. Pimentel, V. L. da Silva, l-Glutamate determination in food samples by flow-injection analysis, Anal. Chim. Acta 448 (2001) 207–213, https://doi.org/10.1016/S0003-2670(01)01326-5.
[4] K. Niaz, E. Zaplatic, J. Spoor, Extensive use of monosodium glutamate: A threat to public health? EXCLI J. 17 (2018) 273–278, https://doi.org/10.17179/excli2018-1092.
[5] F. Aguilar, R. Crebelli, A. di Domenico, B. Dusemund, M.J. Frutos, P. Galtier, D. Gott, U. Gundert-Remy, J.-C. Leblanc, O. Lindtner, P. Moldeus, P. Mosesso, D. Parent-Massin, A. Oskarsson, I. Stankovic, I. Waalkens-Berendsen, R. A. Woutersen, M. Wright, M. Younes, P. Boon, D. Chrysafidis, R. Gürtler, P. Tobback, A. Altieri, A.M. Rincon, C. Lambré, A. Mortensen, Re-evaluation of glutamic acid (E 620), sodium glutamate (E 621), potassium glutamate (E 622), calcium glutamate (E 623), ammonium glutamate (E 624) and magnesium glutamate (E 625) as food additives, EFSA J. 15 (2017), e04910, https://doi.org/10.2903/j.efsa.2017.4910.
[6] G. Hughes, R.M. Pemberton, P.R. Fielden, J.P. Hart, The design, development and application of electrochemical glutamate biosensors, TrAC Trends Anal. Chem. 79 (2016) 106–113, https://doi.org/10.1016/j.trac.2015.10.020.
[7] P. Manusha, S. Yadav, J. Satija, S. Senthilkumar, Designing electrochemical NADH sensor using silver nanoparticles/phenothiazine nanohybrid and investigation on the shape dependent sensing behavior, Sens. Actuators B: Chem. 347 (2021), 130649, https://doi.org/10.1016/j.snb.2021.130649.
[8] V. Lates, D. Gligor, L.M. Muresan, I.C. Popescu, Comparative investigation of NADH electrooxidation at graphite electrodes modified with two new phenothiazine derivatives, J. Electroanal. Chem. 661 (2011) 192–197, https://doi.org/10.1016/j.jelechem.2011.07.046.
[9] C. Gómez-Anquela, M. Revenga-Parra, J.M. Abad, A.G. Marín, J.L. Pau, F. Pariente, J. Piqueras, E. Lorenzo, Electrografting of N′,N′-dimethylphenothiazin-5-ium-3,7-diamine (Azure A) diazonium salt forming electrocatalytic organic films on gold or graphene oxide gold hybrid electrodes, Electrochim. Acta 116 (2014) 59–68, https://doi.org/10.1016/j.electacta.2013.11.021.
[10] M. Revenga-Parra, C. Gómez-Anquela, T. García-Mendiola, E. Gonzalez, F. Pariente, E. Lorenzo, Grafted Azure A modified electrodes as disposable β-nicotinamide adenine dinucleotide sensors, Anal. Chim. Acta 747 (2012) 84–91, https://doi.org/10.1016/j.aca.2012.07.043.
[11] C. Zhu, G. Yang, H. Li, D. Du, Y. Lin, Electrochemical sensors and biosensors based on nanomaterials and nanostructures, Anal. Chem. 87 (2015) 230–249, https://doi.org/10.1021/ac5039863.

[12] E. Martínez-Periñán, M. Revenga-Parra, M. Gennari, F. Pariente, R. Mas-Ballesté, F. Zamora, E. Lorenzo, Insulin sensor based on nanoparticle-decorated multiwalled carbon nanotubes modified electrodes, Sens. Actuators B: Chem. 222 (2016) 331–338, https://doi.org/10.1016/j.snb.2015.08.033.
[13] C. Zhang, X. Du, Electrochemical sensors based on carbon nanomaterial used in diagnosing metabolic disease, Front. Chem. 8 (2020) 651, https://doi.org/10.3389/fchem.2020.00651.
[14] M. Revenga-Parra, A.M. Villa-Manso, M. Briones, E. Mateo-Martí, E. Martínez-Periñán, E. Lorenzo, F. Pariente, Bioelectrocatalytic platforms based on chemically modified nanodiamonds by diazonium salt chemistry, Electrochim. Acta 357 (2020), 136876, https://doi.org/10.1016/j.electacta.2020.136876.
[15] Z. Hassanvand, F. Jalali, M. Nazari, F. Parnianchi, C. Santoro, Carbon nanodots in electrochemical sensors and biosensors: a review, ChemElectroChem 8 (2021) 15–35, https://doi.org/10.1002/celc.202001229.
[16] T. Guerrero-Esteban, C. Gutiérrez-Sánchez, E. Martínez-Periñán, M. Revenga-Parra, F. Pariente, E. Lorenzo, Sensitive glyphosate electrochemiluminescence immunosensor based on electrografted carbon nanodots, Sens. Actuators B: Chem. 330 (2021), 129389, https://doi.org/10.1016/j.snb.2020.129389.
[17] C. Gutiérrez-Sánchez, M. Mediavilla, T. Guerrero-Esteban, M. Revenga-Parra, F. Pariente, E. Lorenzo, Direct covalent immobilization of new nitrogen-doped carbon nanodots by electrografting for sensing applications, Carbon N. Y 159 (2020) 303–310, https://doi.org/10.1016/j.carbon.2019.12.053.
[18] F. Rigodanza, L. Đorđević, F. Arcudi, M. Prato, Customizing the electrochemical properties of carbon nanodots by using quinones in bottom-up synthesis, Angew. Chem. Int. Ed. 57 (2018) 5062–5067, https://doi.org/10.1002/anie.201801707.
[19] Y. Li, X. Zheng, X. Zhang, S. Liu, Q. Pei, M. Zheng, Z. Xie, Porphyrin-based carbon dots for photodynamic therapy of hepatoma, Adv. Healthc. Mater. 6 (2017), 1600924, https://doi.org/10.1002/adhm.201600924.
[20] E. Martínez-Periñán, T. García-Mendiola, E. Enebral-Romero, R. del Caño, M. Vera-Hidalgo, M. Vázquez Sulleiro, C. Navío, F. Pariente, E.M. Pérez, E. Lorenzo, A MoS2 platform and thionine-carbon nanodots for sensitive and selective detection of pathogens, Biosens. Bioelectron. 189 (2021), 113375, https://doi.org/10.1016/j.bios.2021.113375.
[21] M.J. Mostazo-López, R. Ruiz-Rosas, T. Tagaya, Y. Hatakeyama, S. Shiraishi, E. Morallón, D. Cazorla-Amorós, Nitrogen doped superactivated carbons prepared at mild conditions as electrodes for supercapacitors in organic electrolyte, C. (Basel). 6 (2020), https://doi.org/10.3390/c6030056.
[22] D. Liu, W. Lei, D. Portehault, S. Qin, Y. Chen, High N-content holey few-layered graphene electrocatalysts: scalable solvent-less production, J. Mater. Chem. A. 3 (2015) 1682–1687, https://doi.org/10.1039/C4TA05008H.
[23] T. Susi, T. Pichler, P. Ayala, X-ray photoelectron spectroscopy of graphitic carbon nanomaterials doped with heteroatoms, Beilstein J. Nanotechnol. 6 (2015) 177–192, https://doi.org/10.3762/bjnano.6.17.
[24] A.J. Gross, S. Tanaka, C. Colomies, F. Giroud, Y. Nishina, S. Cosnier, S. Tsujimura, M. Holzinger, Diazonium Electrografting vs. Physical Adsorption of Azure A at carbon nanotubes for mediated glucose oxidation with FAD-GDH, ChemElectroChem 7 (2020) 4543–4549, https://doi.org/10.1002/celc.202000953.
[25] C. Priya, G. Sivasankari, S. Sriman Narayanan, Electrochemical behavior of Azure A/gold nanoclusters modified electrode and its application as non-enzymatic hydrogen peroxide sensor, Colloids Surf. B: Biointerfaces 97 (2012) 90–96, https://doi.org/10.1016/j.colsurfb.2012.04.004.
[26] Zbigniew. Galus, Zbigniew. Galus, Fundamentals of electrochemical analysis, (1976).
[27] R. Doaga, T. McCormac, E. Dempsey, Electrochemical sensing of NADH and glutamate based on Meldola Blue in 1,2-Diaminobenzene and 3,4-Ethylenedioxythiophene polymer films, Electroanalysis 21 (2009) 2099–2108, https://doi.org/10.1002/elan.200904627.
[28] S. Chakraborty, C.Retna Raj, Amperometric biosensing of glutamate using carbon nanotube based electrode, Electrochem. Commun. 9 (2007) 1323–1330, https://doi.org/10.1016/j.elecom.2007.01.039.
[29] B. Liang, S. Zhang, Q. Lang, J. Song, L. Han, A. Liu, Amperometric l-glutamate biosensor based on bacterial cell-surface displayed glutamate dehydrogenase, Anal. Chim. Acta 884 (2015) 83–89, https://doi.org/10.1016/j.aca.2015.05.012.
[30] G. Hughes, R.M. Pemberton, P.R. Fielden, J.P. Hart, Development of a novel reagentless, screen-printed amperometric biosensor based on glutamate dehydrogenase and NAD+, integrated with multi-walled carbon nanotubes for the determination of glutamate in food and clinical applications, Sens. Actuators B: Chem. 216 (2015) 614–621, https://doi.org/10.1016/j.snb.2015.04.066.
[31] S.T. Girousi, A.A. Pantazaki, A.N. Voulgaropoulos, Mitochondria-based amperometric biosensor for the determination of L-Glutamic acid, Electroanalysis 13 (2001) 243–245, https://doi.org/10.1002/1521-4109(200103)13:3<243::AID-ELAN243>3.0.CO;2-J.
[32] G. Hughes, R.M. Pemberton, P.R. Fielden, J.P. Hart, Development of a Disposable Screen Printed Amperometric Biosensor Based on Glutamate Dehydrogenase, for the Determination of Glutamate in Clinical and Food Applications Analytical & Bioanalytical Electrochemistry, 2014. ⟨www.abechem.com⟩.
[33] L. Meng, P. Wu, G. Chen, C. Cai, Y. Sun, Z. Yuan, Low potential detection of glutamate based on the electrocatalytic oxidation of NADH at thionine/single-walled carbon nanotubes composite modified electrode, Biosens. Bioelectron. 24 (2009) 1751–1756, https://doi.org/10.1016/j.bios.2008.09.001.
[34] B. Batra, C.S. Pundir, An amperometric glutamate biosensor based on immobilization of glutamate oxidase onto carboxylated multiwalled carbon nanotubes/gold nanoparticles/chitosan composite film modified Au electrode, Biosens. Bioelectron. 47 (2013) 496–501, https://doi.org/10.1016/j.bios.2013.03.063.
[35] X. Wang, J. Duan, Y. Cai, D. Liu, X. Li, Y. Dong, F. Hu, A modified nanocomposite biosensor for quantitative l-glutamate detection in beef, Meat Sci. 168 (2020), 108185, https://doi.org/10.1016/j.meatsci.2020.108185.
[36] A. Mentana, D. Nardiello, C. Palermo, D. Centonze, Accurate glutamate monitoring in foodstuffs by a sensitive and interference-free glutamate oxidase based disposable amperometric biosensor, Anal. Chim. Acta 1115 (2020) 16–22, https://doi.org/10.1016/j.aca.2020.04.020.
[37] J. Chen, Q. Yu, W. Fu, X. Chen, Q. Zhang, S. Dong, H. Chen, S. Zhang, A highly sensitive amperometric glutamate oxidase microbiosensor based on a reduced graphene oxide/prussian blue nanocube/gold nanoparticle composite film-modified Pt electrode, Sensors 20 (2020), https://doi.org/10.3390/s20102924.
[38] D. Maity, R.T.R. Kumar, Highly sensitive amperometric detection of glutamate by glutamic oxidase immobilized Pt nanoparticle decorated multiwalled carbon nanotubes(MWCNTs)/polypyrrole composite, Biosens. Bioelectron. 130 (2019) 307–314, https://doi.org/10.1016/j.bios.2019.02.001.

Emiliano Martínez-Periñán received his bachelor's degree and Master degree in chemistry from Universidad de Cádiz. He obtained his PhD degree from Universidad Autónoma de Madrid in 2016. After that, he had been working as a visiting postdoc researcher at Manchester Metropolitan University under the direction of Professor Craig E. Banks. Then, he obtained a Juan de la Cierva-Formación fellowship from the Spanish Ministry of economy and innovation at the Electroanalysis and Electrochemical Biosensors group of Universidad Complutense de Madrid lead by Professor José Manuel Pingarrón. Nowadays he is working as associated professor in the department of Analytical Chemistry and Instrumental analysis of Universidad Autónoma de Madrid. He is part of the Chemical Sensors and Biosensors group lead by Professor Encarnación Lorenzo. His research interests include electrosynthesis, nanotechnology, the use of different analysis techniques coupled with electrochemistry and electrochemical sensors.

Aitor Domínguez-Saldaña got the degree in chemistry from Universidad Complutense de Madrid in 2019. After that, he received his master's degree in applied chemistry in Universidad Autónoma de Madrid in 2020. In the degree's and master's theses, his main research was the develop of optical and electrochemical sensors and biosensors. In the same year, he began to study a PhD in Sustainable chemistry program of Chemical Technology Institute (Universitat Politècnica de València – CSIC), in the Energy Conversion and Storage Group lead by José Manuel Serra Alfaro. His main PhD research is the microwaves application in catalytic ceramic oxides to storage energy using hydrogen as an energy carrier.

Ana M. Villa-Manso obtained the Degree in Chemistry and the Master Degree in Applied Chemistry in 2018 and 2020, respectively, from the Universidad Autónoma de Madrid. Since this year, she is a PhD student at the Applied Chemistry Programme of the same university in the Chemical Sensors and Biosensors group lead by Professor Encarnación Lorenzo. Her research focuses on the development of nanostructured platforms with emerging nanomaterials for the development of (bio)sensors of analytes of interest.

Cristina Gutiérrez-Sánchez received her PhD degree from UNED in 2012. In the Bioelectrocatalysis laboratory of the Institute of Catalysis, CSIC, under the direction of Dr. Antonio Lopez De Lacey. She worked on the functionalization and characterization of surfaces using different techniques for the development of nanostructured enzyme electrodes. In 2013, she undertook her first postdoctoral contract at the University of Siegen, Germany. Subsequently, she moved to Marseille, France, to the CNRS Bioenergetics and Protein Engineering laboratory, for 2 years. Later, she joined the Bioelectrocatalysis group at the Institute of Catalysis, CSIC in 2016. She is currently working in the group of Chemical Sensors and Biosensors at UAM to carry out the Research Project in the Call for Talent Attraction, modality 1 of the Community of Madrid. Her main research interests include areas as Analytical Chemistry, Bioelectrochemistry, Nanoscience and Materials Science.

Mónica Revenga-Parra obtained the BS degree in Chemistry and Food Science in 2002 and 2005, respectively, from the Universidad Autónoma de Madrid (UAM). She obtained her PhD degree from UAM in 2009. At present, she is associate professor in the Department of Analytical Chemistry and Instrumental Analysis at the UAM. Her research interests include the development of new redox mediators for the design of electrochemical sensors and biosensors and the use of nanomaterials to improve the analytical properties of the developed devices.

Eva Mateo-Martí received her PhD degree on surface science at Leverhulme Centre for Innovative Catalysis, University of Liverpool (UK), Post-Doctoral at Ecole Nationale Superieure de Chimie de Paris (France), and currently permanent Scientific Researcher at Centro de Astrobiologia, Instituto Nacional de T é cnica Aeroespacial in Madrid (Spain). Her main expertise based on spectroscopies applied to surface science studies, planetary simulation chambers and ultra-high vacuum systems. She leads research on reactivity and preservation of biomolecules on surfaces, and its stability due to different environments, searching for spectroscopical fingerprints applied to prebiotic chemistry and planetary exploration. She is a co-author of more than 70 research articles in a wide range of international journals and three patents.

Félix Pariente is currently Full Professor of Analytical Chemistry at the Universidad Autónoma de Madrid (UAM). He was born in Madrid in 1954. He received his B.S. and Ph. D. degrees in Chemistry in 1976 and 1988, respectively. Between 1992 and 1996 he spent several periods as visiting scientist at the University of Cornell in USA. In 1998 he obtains the degree of permanent assistant professor in the UAM. His research interest includes the

design and development of enzyme biosensors and genosensors as well as processes involving electrocatalysis with application to the design of fuel cells and new analytical methods.

María Encarnación Lorenzo is currently Full Professor in the Department of Analytical Chemistry and Instrumental Analysis at the Universidad Autónoma de Madrid. She received her degree in Chemistry in 1978 and her PhD degree in 1985 from the Universidad Autónoma de Madrid. Afterwards, she made a post-doctoral stage at the Department of Chemistry at Dublin City University. In 1990 she was visiting scientist (NATO Program) to the Department of Chemistry in Cornell University. In 1998 the members of the faculty of Tokio University of Agriculture and Technology invited her as visiting professor to the Department of Applied Chemistry. Actually, she is member of management committee of the Spanish Analytical Chemistry Society. Her research interest is the development of sensors and biosensors for the detection of analytes of environmental, clinical and food interest. She is the author/coauthor of more than 100 original research publications and several book chapters in the area of analytical chemistry.